Systemic Anti-CD25 Monoclonal Antibody Administration Safely Enhances Immunity in Murine Glioma without Eliminating Regulatory T Cells

Peter E. Fecci,[2] Alison E. Sweeney,[1] Peter M. Grossi,[1] Smita K. Nair,[1] Christopher A. Learn,[1] Duane A. Mitchell,[1] Xiuyu Cui,[1] Thomas J. Cummings,[2] Darell D. Bigner,[2] Eli Gilboa,[1] and John H. Sampson[1,2]

Abstract

Purpose: Elevated proportions of regulatory T cells (T_{reg}) are present in patients with a variety of cancers, including malignant glioma, yet recapitulative murine models are wanting. We therefore examined T_{regs} in mice bearing malignant glioma and evaluated anti-CD25 as an immunotherapeutic adjunct.

Experimental Design: $CD4^+CD25^+Foxp3^+GITR^+$ T_{regs} were quantified in the peripheral blood, spleens, cervical lymph nodes, and bone marrow of mice bearing malignant glioma. The capacities for systemic anti-CD25 therapy to deplete T_{regs}, enhance lymphocyte function, and generate antiglioma CTL responses were assessed. Lastly, survival and experimental allergic encephalitis risks were evaluated when anti-CD25 was combined with a dendritic cell–based immunization targeting shared tumor and central nervous system antigens.

Results: Similar to patients with malignant glioma, glioma-bearing mice show a CD4 lymphopenia. Additionally, $CD4^+CD25^+Foxp3^+GITR^+$ T_{regs} represent an increased fraction of the remaining peripheral blood $CD4^+$ T cells, despite themselves being reduced in number. Similar trends are observed in cervical lymph node and spleen, but not in bone marrow. Systemic anti-CD25 administration hinders detection of $CD25^+$ cells but fails to completely eliminate T_{regs}, reducing their number only moderately, yet eliminating their suppressive function. This elimination of T_{reg} function permits enhanced lymphocyte proliferative and IFN-γ responses and up to 80% specific lysis of glioma cell targets *in vitro*. When combined with dendritic cell immunization, anti-CD25 elicits tumor rejection in 100% of challenged mice without precipitating experimental allergic encephalitis.

Conclusions: Systemic anti-CD25 administration does not entirely eliminate T_{regs} but does prevent T_{reg} function. This leads to safe enhancement of tumor immunity in a murine glioma model that recapitulates the tumor-induced changes to the CD4 and T_{reg} compartments seen in patients with malignant glioma.

It is currently well established that the peripheral $CD4^+$ T-cell repertoire is equipped with its own means for the enforcement of tolerance (1–9). Focused within the $CD25^+GITR^+Foxp3^+$ compartment (10, 11), this regulatory T-cell constituent (T_{reg}) also seems to play a significant role in hindering immunity to tumor antigens (12, 13). Accordingly, T_{regs} come to represent an increased fraction of $CD4^+$ T cells in the peripheral blood or tumor of patients with a variety of malignancies (13–16). Recent work also indicates that such increased "T_{reg} fractions" exist amidst severe CD4 lymphopenia in patients harboring malignant glioma (17) and assume responsibility for cellular immune defects described for these patients over the last three decades (reviewed in ref. 18). Therefore, provided an appropriate, recapitulative murine model of malignant glioma, targeting T_{reg} activity could gain justification as a means to counter immunosuppression and enhance antitumor immune responses in these patients. This strategy currently remains untested in brain tumor models.

We report here that our murine model of glioma indeed recapitulates malignant glioma–induced changes to the human peripheral blood CD4 and T_{reg} compartments. Specifically, tumor-bearing mice exhibit CD4 lymphopenia whereas $CD4^+CD25^+Foxp3^+GITR^+$ T_{regs} come to represent an increased fraction of the peripheral blood $CD4^+$ T cells that remain despite themselves being reduced in number. Extending the study to other sites, similar phenomena are observed in the spleens and cervical lymph nodes whereas the reverse scenario emerges in bone marrow.

Authors' Affiliations: [1]Division of Neurosurgery, Department of Surgery and [2]Department of Pathology, Duke University Medical Center, Durham, North Carolina
Received 1/9/06; revised 4/12/06; accepted 4/20/06.

Grant support: NIH Specialized Program of Research Excellence grants 1P50 CA108786 (D.D. Bigner and J.H. Sampson), R01 CA09722 (J.H. Sampson), and MSTP T32 GM-07171 (P.E. Fecci); the Brain Tumor Society (J.H. Sampson); Accelerate Brain Cancer Cure Foundation (J.H. Sampson and D.D. Bigner); and NIH award AI-51445 (Duke Human Vaccine Institute Flow Cytometry Core Facility). The costs of publication of this article were defrayed in part by the payment of page charges. This article must therefore be hereby marked *advertisement* in accordance with 18 U.S.C. Section 1734 solely to indicate this fact.

Requests for reprints: John H. Sampson, Division of Neurosurgery, Department of Surgery, Duke University Medical Center, Durham, NC 27710. Phone: 919-684-9041; Fax: 919-684-9045; E-mail: john.sampson@duke.edu.

doi:10.1158/1078-0432.CCR-06-0053

We employed this model to investigate the *in vivo* effects of T_{reg} removal on antiglioma immune responses. The current doctrine is that effective depletion of T_{regs} may be achieved simply by systemic administration of anti-CD25 monoclonal antibody (mAb; refs. 19–21). Likewise, in non–central nervous system (CNS) tumor models, the administration of anti-CD25 mAb has been employed in attempts to remove T_{regs} and has effectively elicited prolonged survival to s.c. tumor challenge (22–24). These studies, however, predated our ability to examine Foxp3 expression in T_{regs} with antibody staining.

Following *in vivo* administration of anti-CD25 mAb, we discovered that $CD4^+Foxp3^+GITR^+$ cells failed to entirely disappear despite the present thinking. Instead, they persisted at significant levels in all sites tested. When isolated based on CD4 and glucocorticoid-induced tumor necrosis factor–like receptor (GITR) expression, however, these cells showed none of the typical suppressive capacities of $CD4^+CD25^+GITR^+$ T_{regs} *in vitro*. Accordingly, systemic anti-CD25 mAb proved capable of enhancing T-cell proliferation, IFN-γ production, and glioma-specific CTL responses in treated mice. When combined with a dendritic cell–based immunization strategy, anti-CD25 mAb elicited glioma rejection in 100% of challenged mice without attendant induction of experimental allergic encephalitis. Systemic anti-CD25 mAb administration therefore seems to counter the suppressive effects of T_{regs} without comprehensively eliminating the cells *in vivo*. This activity proves permissive for potent antitumor immunity in a murine glioma model that aptly recapitulates tumor-induced changes to the CD4 and T_{reg} compartments.

Materials and Methods

Tumor cell line and experimental animals. The SMA-560 cell line was derived from a spontaneous intracerebral malignant glioma arising in inbred VM/Dk mice. VM/Dk mice were obtained from the McLaughlin Research Institute (Great Falls, MT) and an inbred colony was established at Duke University. Mice are maintained in a pathogen-free environment.

Antibodies. Antibodies to CD3 (145-2C11), CD4 (L3T4), CD16/32 (2.4G2), CD25 (PC61 and 7D4), and rat immunoglobulin G1 (IgG1) and appropriate isotype controls were obtained from BD PharMingen (San Diego, CA). Anti-α-GITR (108619) was obtained from R&D Systems (Minneapolis, MN) and α-Foxp3 (FJK-16s) was obtained from eBioscience (San Diego, CA). Anti-CD25 (PC61) ascites for *in vivo* administration was obtained from Accurate Chemical (Westbury, NY).

Flow cytometry. Spleens and cervical lymph nodes were harvested, minced, and pushed through cell screens to create single-cell suspensions. Whole blood was obtained by retro-orbital bleed. Bone marrow was harvested from tibias. RBC lysis was done on spleens, bone marrow, and whole blood as needed with 1× ammonium chloride lysing solution (BD PharMingen). Cells were incubated first with antibodies against surface markers for 30 minutes at 4°C in the dark. Cells were fixed and permeabilized using 1× Fix/Perm solution (eBioscience) according to the instructions of the manufacturer. Following incubation period, cells were washed in 1× Permeabilization Buffer (eBioscience), Fc-blocked with α-CD16/32, and stained with α-Foxp3 for 30 minutes at 4°C in the dark. Cells were washed, fixed, and analyzed on a FACSVantage SE or LSRII flow cytometer (BD Biosciences).

Isolation of T cells and T_{regs}. Spleen and cervical lymph node cells were harvested as above. Miltenyi mouse $CD4^+$ Isolation Kit (Miltenyi Biotec, Auburn, CA) was used to isolate $CD4^+$ cells, without engaging the CD4 molecule, according to the instructions of the manufacturer. Briefly, a biotinylated antibody cocktail specific for non-$CD4^+$ cells (CD8a, CD11b, CD45R, DX5, and Ter119) was added at 10 μL/10^7 cells. Samples were incubated and then mixed with antibiotin microbeads. Samples were reincubated, washed, and run over AUTOMACS (Miltenyi) set to program DEPLETE. Unless otherwise indicated, nonlabeled fraction ($CD4^+$) was counted, labeled with allophycocyanin-α-CD25 and phycoerythrin-α-GITR, and sorted into $CD25^+GITR^+$ and $CD25^-$ populations on a FACSVantage SE flow cytometer (BD Biosciences). Purity of each population was always >98% to 99%.

T-cell cultures. For proliferation and suppression assays, cells were cultured in triplicate in 96-well plates and stimulated with either soluble or plate-bound α-CD3e antibody (145-2C11; BD PharMingen) at 2 μg/mL. $CD4^+CD25^-$ and $CD4^+CD25^+GITR^+$ cells (unless otherwise indicated) were purified as above from VM/Dk mice. Cells were cultured alone or mixed in varying proportions in triplicate wells in 200 μL T-cell medium consisting of RPMI 1640 + 10% FCS, supplemented with HEPES buffer, sodium pyruvate, penicillin/streptomycin, L-glutamine, β-mercaptoethanol, and nonessential amino acids (all from Life Technologies, Inc., Grand Island, NY).

For T-cell proliferative responses following *in vivo* T_{reg} depletion, spleens were harvested 5 days after depletion as above. Nonadherent cells were plated in triplicate wells in T-cell medium alone or mixed 1:1 with 5-μm latex beads (Interfacial Dynamics, Tualatin, OR) coated with α-CD3e (145-2C11) and α-CD28 (clone 37.51, BD PharMingen).

Measurement of proliferation. In all cases, after 72 hours of culture, 1 μCi [^{3}H]thymidine (Amersham, Piscataway, NJ) was added to each well. Cells were cultured for an additional 16 hours and then harvested on a FilterMate cell harvester (Perkin-Elmer, Boston, MA). [^{3}H] counts were done using a Wallac 1450 Microbeta Trilux Liquid Scintillation/Luminescence Counter (Perkin-Elmer). Data were taken as means of triplicate wells.

IFN-γ ELISA. Experimental supernatants were assayed for IFN-γ levels using eBioscience IFN-γ ELISA sets (eBioscience) according to the instructions of the manufacturer. Briefly, ELISA plates were coated with capture antibody and incubated overnight at 4°C. The following day, wells were washed and blocked before addition of standards and samples to the appropriate wells. Plates were later incubated with detection antibody and detected with avidin-horseradish peroxidase, followed by addition of substrate and stop solutions. Plates were read at 450 nm.

Generation of murine bone marrow–derived dendritic cells. Tibias, femurs, and sternums were removed using sterile technique and marrow was harvested. RBCs were lysed with ammonium chloride. Cells were suspended in complete dendritic cell medium and plated in six-well plates. Dendritic cell medium consists of T-cell medium + 18 ng/mL murine granulocyte-macrophage colony-stimulating factor (Peprotech, Rocky Hill, NJ) + 18 ng/mL murine interleukin 4 (Peprotech). Medium was replaced on day 3. On day 7, nonadherent cells were collected and replated. On day 8, nonadherent cells were harvested and electroporated with total tumor RNA isolated from the SMA-560 glioma cell line using RNeasy Midi Kit (Qiagen, Valencia, CA) at 300 V × 500 μs using an ECM 830 electroporator (BTX, San Diego, CA). On day 9, nonadherent cells were harvested for use in vaccines.

CTL assay. Target cells (5×10^6-10×10^6) were labeled with europium for 20 minutes at 4°C. Europium-labeled targets (10^4) and serial dilutions of effector cells at varying effector/target ratios were incubated in T-cell medium for 4 hours. Supernatant was harvested and europium release was measured by time-resolved fluorescence. Specific cytotoxic activity was determined using the following formula: % specific release = [(experimental release − spontaneous release) / (total release − spontaneous release)] × 100. Spontaneous release of the target cells was <25% of total release by detergent in all assays. SE of triplicate cultures was <5%.

Intracranial tumor challenge. Tumor cells were harvested, mixed with an equal volume of 10% methylcellulose in PBS, and loaded into

250-μL Hamilton syringes (Hamilton, Reno, NV). Mice (VM/Dk or athymic BALB/c) were anesthetized with a mixture of xylazine/ketamine and placed into a stereotactic frame (Kopf Instruments, Tujunga, CA). The injection needle was positioned 2 mm to the right of bregma and 4 mm below the surface of the skull. Cells (1.0×10^4) in a volume of 5 μL were delivered into the right cerebral hemisphere. After injection, the skull hole was closed with bone wax and the wound was closed with surgical staples (Stoelting Co., Wood Dale, IL).

Experimental allergic encephalitis induction and evaluation. VM/Dk mice were immunized i.d. in the left groin with 100 μL of an emulsion composed of myelin oligodendrocyte glycoprotein 35-55 (MOG35-55) peptide (200 μg/mouse) in PBS and an equal volume of complete Freund's adjuvant (Difco, Detroit, MI). Mice were checked daily for signs of experimental allergic encephalitis. The clinical severity of experimental allergic encephalitis was graded into six categories: grade 0, no sign; grade 1, tail paralysis; grade 2, mild hind limb weakness; grade 3, moderate to severe hind limb paresis and/or mild forelimb weakness; grade 4, complete hind limb paralysis and/or moderate to severe forelimb weakness; grade 5, quadriplegia or moribund; and grade 6, death. Brains and spinal cords were sectioned and stained with H&E and luxol fast blue. Slides were evaluated for evidence of lymphocytic infiltrates and demyelination.

Statistical analysis. Unless otherwise stated, comparisons of T-cell numbers, T_{reg} fractions, and proliferation levels among groups were made using unpaired *t* tests. To compare lysis curves generated in CTL assays, a generalized linear model for normal data that accounted for correlation of measurement replication within groups was used. Survival estimates and median survivals were determined using the method of Kaplan and Meier. Survival curves for each group were compared using the log-rank test.

Results

Validation of T_{reg} phenotype and function in normal and tumor-bearing mice. T_{regs} were defined phenotypically as $CD4^+$ T cells coexpressing the surface markers CD25 and GITR, as well as the intracellular T_{reg}-specific transcription factor forkhead box p3 (Foxp3). Using flow cytometry, we validated that Foxp3 was found specifically within those $CD4^+$ T cells expressing both CD25 and GITR. A representative analysis is depicted in Fig. 1A. These analyses were done in peripheral blood, cervical lymph node, spleen, and bone marrow. Nearly all $CD4^+CD25^+GITR^+$ T cells present at each site were $Foxp3^+$ (spleen, 87%; lymph node, 97%; whole blood, 90%; bone marrow, 86%). This was true in naïve and tumor-bearing mice alike, indicating that the vast majority of $CD4^+CD25^+GITR^+$ T cells present at each site in mice bearing glioma were T_{regs} and not activated T cells (Fig. 1B). This finding also permitted us to use a $CD4^+CD25^+GITR^+$ surface phenotype for T_{regs} when sorting cells for entry into subsequent functional validation experiments (sorting based on Foxp3, which is intracellular, is not possible if viable cells are required).

To obtain functional validation then, $CD4^+CD25^+GITR^+$ T cells present in both naïve and tumor-bearing mice were sorted and tested in standard *in vitro* assays. We confirmed that $CD4^+CD25^+GITR^+$ T cells in both naïve and tumor-bearing mice were anergic to T-cell receptor stimulation and exhibited a dose-dependent capacity to suppress the proliferation of surrounding $CD4^+CD25^-$ T cells.

To this end, $CD4^+$ T cells were enriched through negative selection (leaving the CD4 molecule untouched) and were sorted into $CD25^+GITR^+$ and $CD25^-$ populations. The abilities of each population to proliferate in response to anti-CD3 ± anti-CD28 mAbs were tested, and whereas $CD4^+CD25^-$ cells in all instances proliferated well, $CD4^+CD25^+GITR^+$ cells from tumor-bearing mice failed to respond, in a manner identical to those isolated from naïve mice (Fig. 1C). Furthermore, $CD4^+CD25^+GITR^+$ cells from each group exhibited comparable dose-dependent capacities to suppress the proliferative responses of a fixed number of $CD4^+CD25^-$ cells (Fig. 1D). The use of a fixed number of responders in these assays ruled out the prospect of a dilutional effect due to addition of nonresponsive T_{regs} and likewise indicated true suppressive activity.

Alterations to the T_{reg} and CD4 compartments in mice bearing glioma. Patients with malignant glioma show a markedly increased T_{reg} fraction in their peripheral blood, which serves to hinder their cellular immune responses (17). We therefore evaluated the T_{reg} fraction in mice harboring intracranial SMA-560 glioma. T_{reg} fraction was defined *a priori* as the percentage of $CD4^+$ T cells coexpressing CD25, GITR, and Foxp3. In addition to peripheral blood, however, T_{reg} fraction was also analyzed in the cervical lymph nodes, spleens, and bone marrow of naïve VM/Dk mice, as well as of VM/Dk mice implanted intracranially 21 days earlier with 10,000 SMA-560 glioma cells. Median survival following this manner of implantation is typically 24 to 27 days (data not shown).

The T_{reg} fraction assessed in the peripheral blood of naïve mice was 2.61 ± 0.17% of $CD4^+$ T cells (mean ± SE; $n = 10$). In VM/Dk mice bearing malignant glioma, however, this fraction was raised by 65% to 4.31% ± 0.34% ($n = 10$, $P = 0.0004$; Fig. 2A). Elevations in T_{reg} fraction were also found in the cervical lymph nodes of tumor-bearing mice (Fig. 2A). As tumors were implanted within the right cerebral hemisphere, however, T_{reg} fractions in the ipsilateral (right) and contralateral (left) cervical lymph nodes were measured individually. In general, T_{regs} represented a larger proportion of $CD4^+$ T cells in cervical lymph nodes than in peripheral blood (mean T_{reg} fraction in cervical lymph nodes of naïve mice was 9.51 ± 0.26%, $n = 20$, versus 2.61% ± 0.17% in peripheral blood, $P < 0.0001$). As expected, no significant differences were observed between the left and right cervical lymph nodes of naïve mice ($P = 0.548$). Whereas the T_{reg} fraction was elevated bilaterally in the cervical lymph nodes of tumor-bearing mice relative to naïve mice, however (Fig. 2A), in tumor-bearing mice this elevation was significantly higher within ipsilateral nodes, where T_{reg} fraction reached as high as 37% (mean, 21.94 ± 2.67%; $P = 0.011$). A representative staining from the ipsilateral cervical lymph nodes is depicted in Fig. 2B. In the spleen, a small but nonsignificant increase in T_{reg} fraction was also observed among mice bearing tumor (naïve, 9.83 ± 1.02%; tumor-bearing, 10.83 ± 1.30%; $P = 0.567$; Fig. 2A).

Interestingly, whereas increases in T_{reg} fraction were observed in the tissues above, a decrease in T_{reg} fraction was observed within the bone marrow of mice bearing glioma. Notably, in naïve mice, T_{regs} represented a disproportionately large percentage of $CD4^+$ T cells present (mean, 40.70 ± 1.07%) as compared with the other sites evaluated. In tumor-bearing mice, however, this value dropped precipitously, such that T_{regs} came to represent only 16.92 ± 3.42% of $CD4^+$ T cells ($P = 0.0021$; Fig. 2A). A representative analysis of bone marrow is depicted in Fig. 2C.

We also sought to determine the relative presence of T_{regs} at the tumor site in mice with glioma. To this end, SMA-560 tumors were isolated from VM/DK mice 21 days following

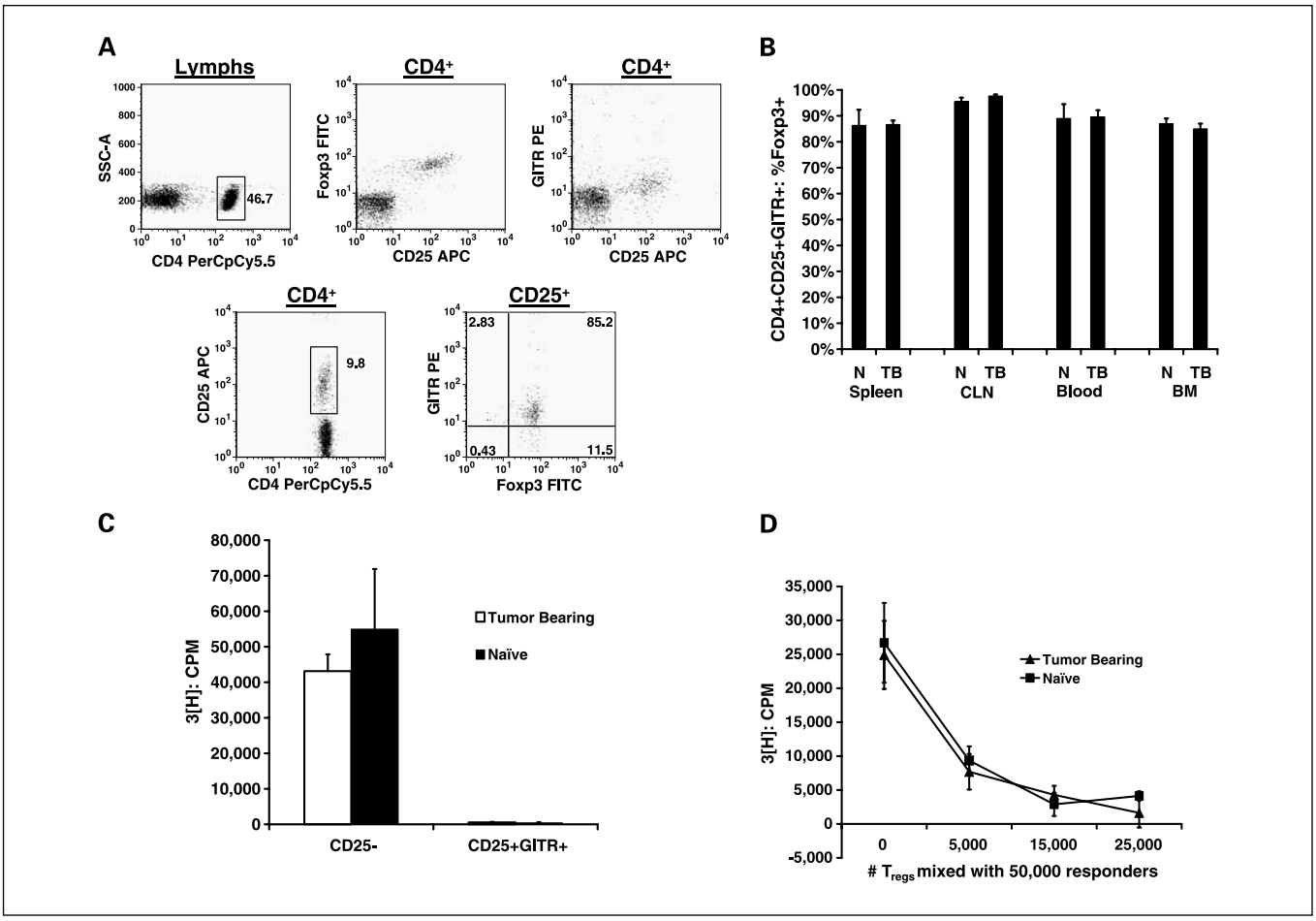

Fig. 1. Verification of T_{reg} phenotype and function. *A,* Foxp3 is found specifically in $CD4^+CD25^+GITR^+$ cells. Representative analyses are shown. First image shows gating of $CD4^+$ lymphocytes. Expression of CD25 × Foxp3 and CD25 × GITR in these cells is depicted in second and third images, respectively. Fourth image shows further gating of $CD25^+$ cells, and fifth image shows GITR × Foxp3 expression on these $CD4^+CD25^+$ cells. Tissue depicted is cervical lymph nodes. Results were similar for peripheral blood and spleen. *B,* comparison of Foxp3 levels in $CD4^+CD25^+GITR^+$ lymphocytes in the spleen, cervical lymph nodes, and peripheral blood of naïve and tumor-bearing animals. The percent $Foxp3^+$ staining is depicted. No differences between normal and tumor-bearing animals are observed. *C,* proliferation assay showing relative T_{reg} anergy. $CD4^+$ cells were isolated and sorted into $CD25^-$ and $CD25^+GITR^+$ populations. $CD25^-$ cells (100,000) or $CD25^+GITR^+$ cells (100,000) were cultured with 2 μg/mL anti-CD3 as stimulator. Proliferation was assessed via $[^3H]$thymidine uptake. Columns, mean counts over triplicate wells. T_{regs} from both naïve and tumor bearing mice showed relative anergy. *D,* T_{reg} suppression assay. The ability of increasing doses of $CD4^+CD25^+GITR^+$ T_{regs} to suppress the proliferation of 5×10^4 $CD4^+CD25^-$ responder cells is represented. T_{regs} were added at doses of 0; 5,000; 10,000; 15,000; and 25,000. Proliferation was assessed via $[^3H]$thymidine uptake. Points, mean counts over triplicate wells. T_{regs} from both naïve and tumor-bearing mice showed requisite suppressive capacity.

tumor implantation. Samples were fixed, paraffin embedded, and subsequently examined by immunohistochemistry for Foxp3. Surrounding normal brain and SMA-560 tumors likewise isolated from athymic BALB/c mice served as controls. Scattered $Foxp3^+$ cells were found exclusively within the tumors of immunocompetent mice, confirming a T_{reg} infiltration of murine gliomas (Fig. 2D).

In patients with malignant glioma, increases in the peripheral blood T_{reg} fraction exist amidst a dramatic CD4 lymphopenia. Consequently, the absolute number of peripheral blood T_{regs} in these patients is actually reduced (17). We therefore assessed the absolute CD4 and T_{reg} counts in the peripheral blood, cervical lymph node, spleen, and bone marrow of glioma-bearing (day 21) versus naïve mice. Complete blood cell, total cervical lymph node cell, total splenocyte, and total tibial bone marrow cell counts were determined and cells were subjected to flow cytometric analysis. Live-cell and lymphocyte gates were created on forward and side scatter plots and the percentages of cells that represented viable $CD3^+$, $CD3^+CD4^+$, and $CD4^+CD25^+Foxp3^+GITR^+$ lymphocytes were subsequently determined. These percentages were multiplied by total cell counts to determine absolute counts of the respective cells and these counts were compared among groups.

As may be observed in Fig. 3A and Table 1, the presence of SMA-560 within the intracranial compartment elicited dramatic reductions in the number of $CD4^+$ T cells in both the ipsilateral and contralateral cervical lymph nodes ($P = 0.001$ and $P = 0.002$, respectively). This was especially pronounced in the ipsilateral cervical lymph nodes ($P = 0.014$ for comparison with contralateral cervical lymph nodes). Similar decreases were also present in the spleen and peripheral blood.

Absolute counts of T_{regs} were subsequently quantified in the same locations. Despite representing an increased fraction of $CD4^+$ T cells in both the peripheral blood and cervical lymph nodes of tumor-bearing mice (Fig. 2A), T_{regs} in these mice were reduced in absolute number at each site (Fig. 3B). The decreases in the cervical lymph nodes were significant (ipsilateral,

$P < 0.0001$; contralateral, $P < 0.0001$). In the spleens of glioma-bearing mice, where T_{regs} had not exhibited a significantly increased representation among $CD4^+$ T cells (Fig. 2A), absolute reductions were also present and were indeed significant (naïve, 2,113,465 ± 90,120; tumor-bearing, 433,099 ± 105,100; $P < 0.0001$; Fig. 3B). At none of the above sites then were T_{regs} observed to have actually expanded in number in the tumor-bearing state.

Interestingly, the opposite scenario was observed in the bone marrow. Although no significant differences in total bone marrow cell counts were observed among naïve and tumor-bearing mice ($P = 0.3118$; data not shown), $CD4^+$ T cells came to be present at both increased percentages [$P = 0.0024$; observed in Fig. 2C (*left*)] and increased numbers ($P = 0.002$; Fig. 3C) in the marrow of mice harboring glioma. These increases were dramatic, approaching and exceeding 400%, respectively. Accordingly, despite exhibiting diminished T_{reg} fractions in the bone marrow, glioma-bearing mice showed a nearly 70% increase in the absolute number of T_{regs} present in this compartment ($P = 0.011$; Fig. 3C). A more striking and disproportionate increase, however, was thus observed in the absolute number of $CD4^+CD25^-$ cells, which were expanded >6-fold in the marrow of tumor-bearing mice ($P = 0.002$; Fig. 3C). Therefore, whereas $CD4^+$ T cells and T_{regs} were found to be reduced in absolute number in the peripheral blood, cervical lymph nodes, and spleen of tumor-bearing mice, these cells were conversely found at greater numbers in the bone marrow of the same animals.

Administration of anti-CD25* in vivo *disrupts T_{reg} function without eliciting a complete T_{reg} depletion. Given the ability of T_{regs} to influence immune responses in patients with malignant glioma, we wished to evaluate the effects of *in vivo* anti-CD25 administration on immune responses in our recapitulative murine model. It has been widely supposed, including by us, that administration of anti-CD25 antibody *in vivo* results in the long-lived depletion of $CD25^+$ T_{regs}, thus permitting enhanced T-cell responses (19). The availability of mAbs to Foxp3, however, now permits us to more closely follow the fate of T_{regs}

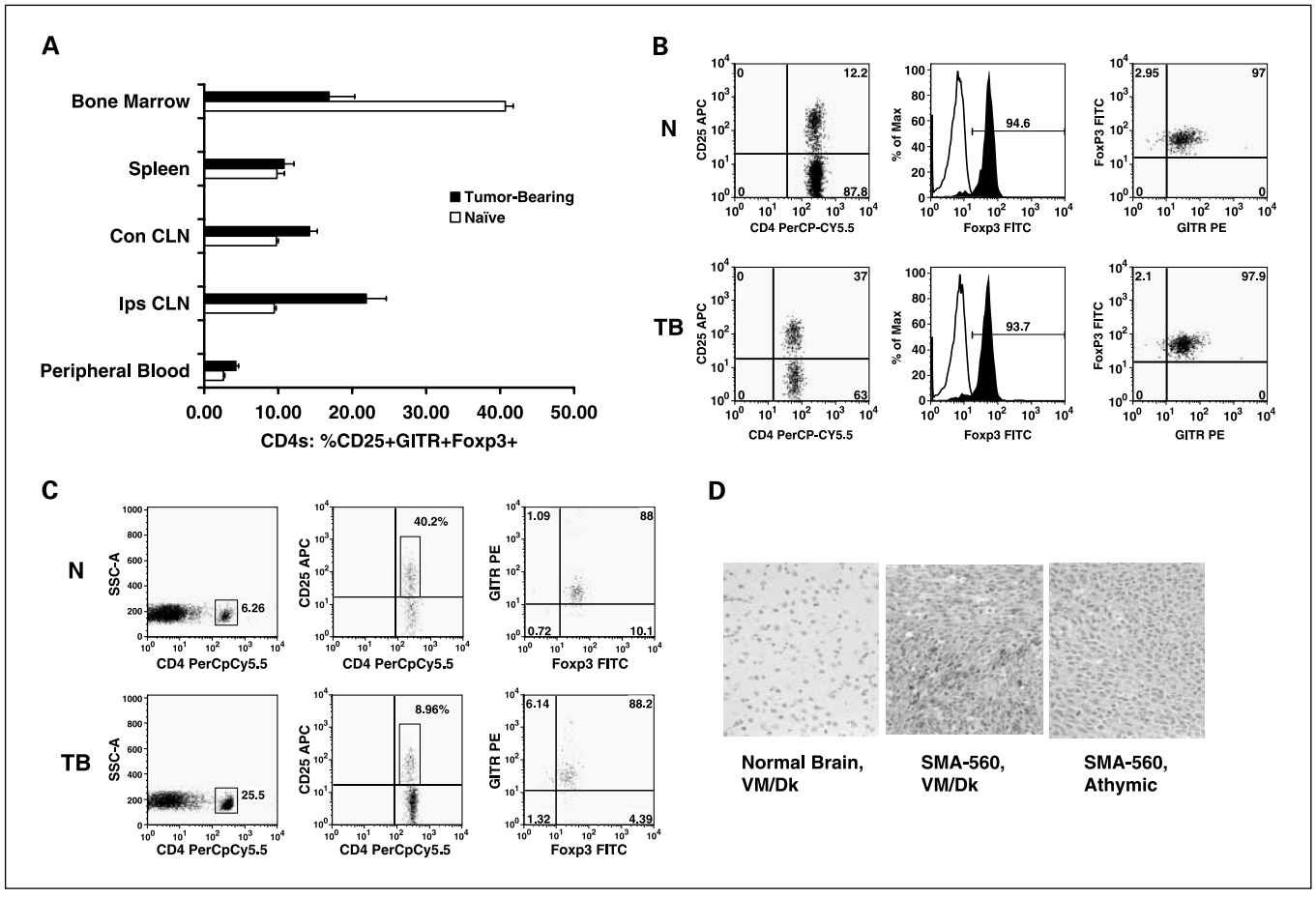

Fig. 2. Measurement of T_{reg} fraction. *A*, T_{reg} fraction (percent $CD4^+$ lymphocytes that are $CD25^+Foxp3^+GITR^+$) in peripheral blood, cervical lymph nodes, spleen, and bone marrow of naïve mice ($n = 10$) and mice with intracranial glioma (tumor-bearing; $n = 10$). Significant elevations are found in the blood ($P = 0.0004$), ipsilateral cervical lymph nodes ($P = 0.01$), and contralateral cervical lymph nodes ($P = 0.008$) of tumor-bearing mice. Furthermore, within tumor-bearing mice, ipsilateral cervical lymph nodes exhibit a higher T_{reg} fraction than contralateral cervical lymph nodes ($P = 0.011$). In contrast, a decrease in T_{reg} fraction was observed within the bone marrow of tumor-bearing mice ($P = 0.0021$). Columns, mean; bars, SE. Comparisons between groups were made using unpaired *t* tests. *B*, representative analysis of CD25, Foxp3, and GITR levels in ipsilateral (right) cervical lymph nodes isolated from naïve (*N*) and tumor-bearing (*TB*) mice. Left, gated on $CD4^+$ lymphocytes and depict CD4 × CD25 staining. Middle, levels of Foxp3 in $CD4^+CD25^+$ (■) and $CD4^+CD25^-$ (□) cells. Right, gated on the $Foxp3^+$ cells, as shown, and render GITR × Foxp3 staining. *C*, alternative analysis depicting representative scenarios in bone marrow of naïve and tumor-bearing mice. Left, cells pulled through a lymphocyte forward and side scatter gate and further CD4 gating. Increased percentages of $CD4^+$ cells are found in tumor-bearing mice. Middle, $CD4^+$ cells and the percentage of $CD25^+$ cells (decreased in TB mice), which are also subsequently gated; right, levels of Foxp3 and GITR on these $CD25^+$ cells. *D*, T_{regs} are found at the tumor site, as tumor-infiltrating lymphocytes (not found in athymic mice harboring tumor) stain positively for Foxp3 by immunohistochemistry.

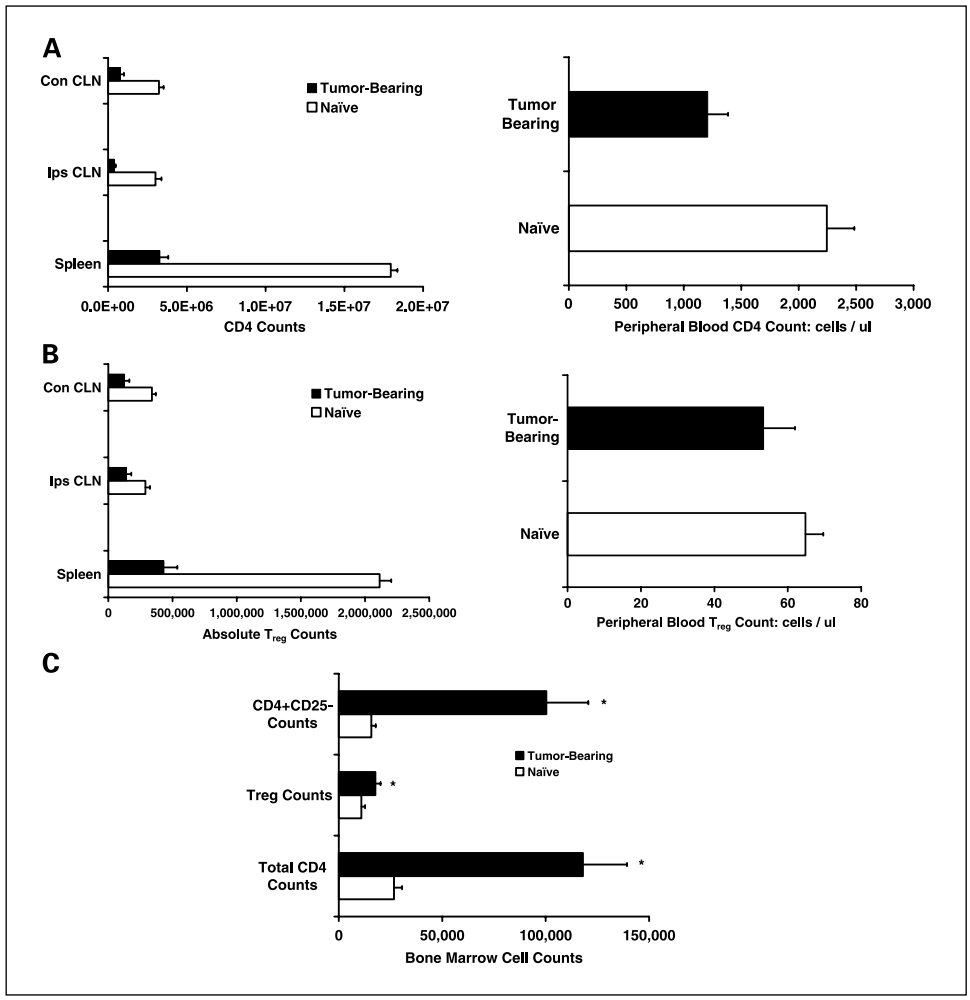

Fig. 3. Absolute CD4 and T_{reg} counts. *A* and *B,* counts in cervical lymph node, spleen, and peripheral blood. Absolute counts of $CD4^+$ T cells (*A*) and T_{regs} (*B*) are shown for the cervical lymph nodes (*left*), spleens (*left*), and peripheral blood (*right*) of tumor-bearing versus naïve mice. At these sites, CD4 counts were dramatically reduced (see Table 1). T_{regs}, despite generally representing an increased percentage of $CD4^+$ T cells in these locations, were also typically reduced in number. Decreases in the ipsilateral cervical lymph nodes, contralateral cervical lymph nodes, and spleen of tumor-bearing mice were significant when compared with the same sites in naïve mice using unpaired *t* tests ($P < 0.0001$ for each location). *C,* CD4 and T_{reg} counts in bone marrow. Unlike the situation at other sites, both $CD4^+$ T cells ($P = 0.002$) and T_{regs} ($P = 0.011$) were found in greater numbers within the bone marrow of tumor-bearing mice. T_{regs} increased their presence by ~70% despite representing a dramatically reduced fraction of $CD4^+$ T cells. This contrast may be explained by the >6-fold increase in $CD4^+CD25^-$ T-cell counts ($P = 0.002$) in the bone marrow of glioma-bearing mice, also depicted in (*C*).

in mice following administration of anti-CD25. Accordingly, we examined the time course of CD4, CD25, Foxp3, and GITR levels in mice given a single i.p. injection of anti-CD25 (PC61) mAb. We found, in agreement with very recent work by Kohm et al. (25), that anti-CD25 may not work entirely by eliminating T_{regs}, as originally thought.

Following administration of 0.5 mg anti-CD25 ascites (PC61), VM/Dk mice were sacrificed at various time points, and the levels of $CD4^+CD25^+$ and $CD4^+Foxp3^+GITR^+$ cells assessed independently by flow cytometry. Measurements were taken in the peripheral blood, cervical lymph node, spleen, and bone marrow. As may be observed in Fig. 4A, CD25 (PC61) became rapidly undetectable on the surface of cells at all sites following antibody administration and levels did not begin to recover for ~40 days.

In contrast, in the days following anti-CD25 administration, $CD4^+Foxp3^+GITR^+$ T cells remained detectable at all sites evaluated (Fig. 4A). A moderate decrease in their levels was observed over time, and this change generally reached a plateau before a gradual recovery initiated. These results suggested to us

Table 1. Mean CD4 counts in naïve and tumor-bearing mice

	Naïve	Tumor-bearing	*P* for comparison
Ipsilateral cervical lymph nodes	3,007,265	387,275	0.001
Contralateral cervical lymph nodes	3,232,272	769,396	0.002
Spleen	17,950,868	3,282,728	<0.0001
Peripheral blood (cells/μL)	2,245	1,209	0.0045
Bone marrow (per tibia)	26,662	117,990	0.002

NOTE: Differences at all sites measured are significant as indicated by the included *P* values. Additionally, differences between ipsilateral and contralateral cervical lymph nodes within tumor-bearing mice are significant ($P = 0.014$), with ipsilateral cervical lymph nodes showing greater reduction in counts.

that T_{regs} in fact persisted at some level at each site; it seemed dramatically less likely that a population of $CD4^+CD25^-$ $Foxp3^+GITR^+$ cells had instead arisen *de novo*.

To examine this further, however, we analyzed the levels of CD4, Foxp3, GITR, and two epitopes of CD25 (PC61 and 7D4) present in the lymphocytes of mice in the minutes and hours immediately following *in vivo* PC61 administration. Furthermore, as the administered PC61 antibody is a rat IgG1 isotype, we assessed the levels of rat IgG1 present on the surface of cells over the same time periods (Fig. 4B). We found that although levels of CD25 detected with the same PC61 clone rapidly declined (<45 minutes), CD25 levels detected with a different anti-CD25 clone, 7D4, remained at normal levels for nearly 24 hours. These levels then began a gradual decline that mimicked exactly the time course of Foxp3 levels. Additionally, whereas rat IgG1 was not detectable on the surface of cells before *in vivo* PC61 administration, by 45 minutes after injection, its levels matched those of Foxp3 and 7D4, a pattern that continued out to 40 days. Both 7D4 and rat IgG1 were found specifically on the surface of $Foxp3^+$ and $GITR^+$ cells (correlative surface presence of rat IgG1 and GITR shown in Fig. 4C). Together, these data strongly suggest that the

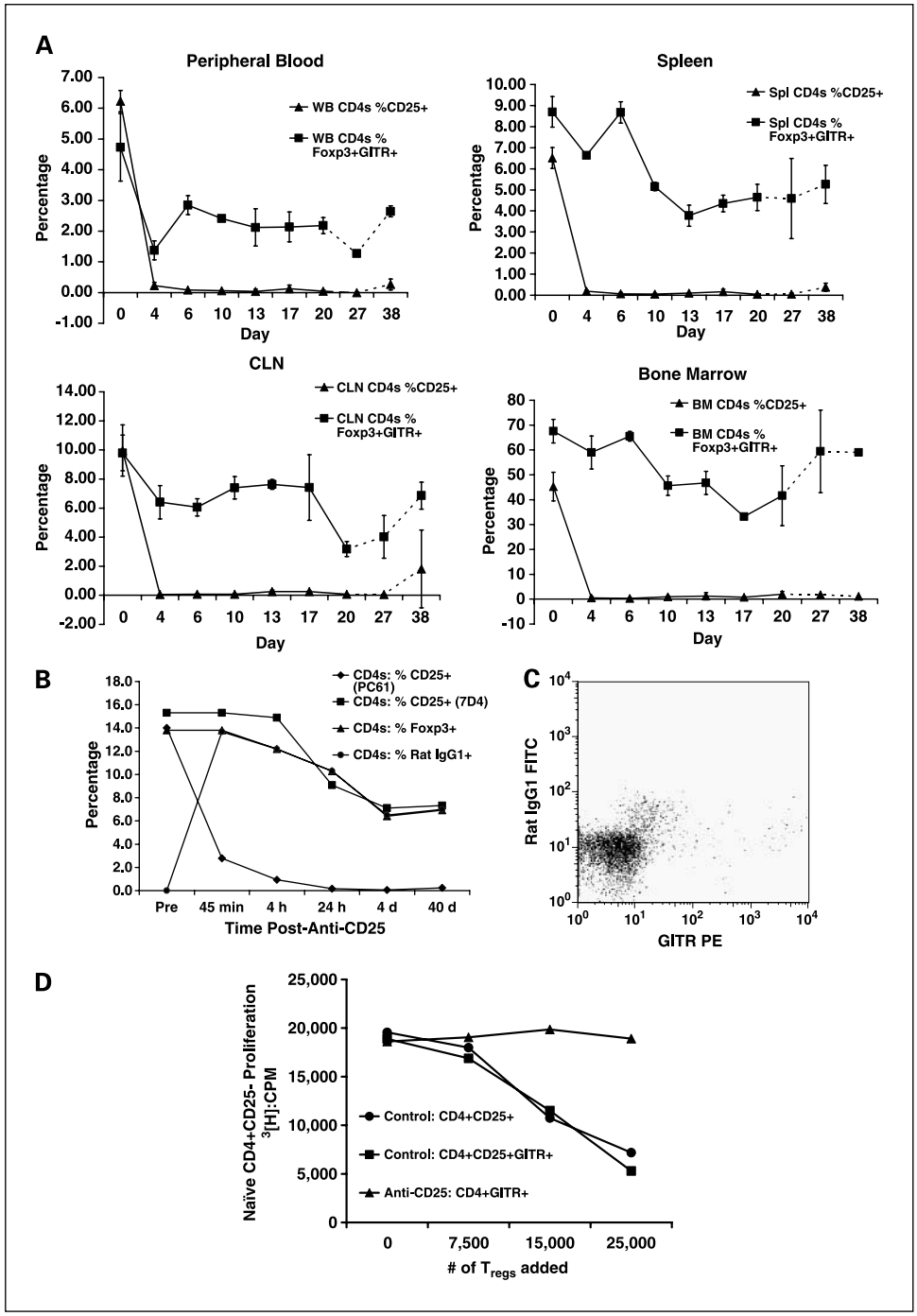

Fig. 4. Systemic anti-CD25 fails to eliminate $CD4^+Foxp3^+GITR^+$ cells but interferes with their suppressive function. *A,* relative percentages of $CD4^+$ T cells in which CD25 (PC61) or Foxp3 and GITR are detectable in the days following *in vivo* anti-CD25 (PC61) administration. Although CD25 becomes rapidly undetectable, $CD4^+Foxp3^+GITR^+$ cells experience only a slow and moderate decline. *B,* time curves of CD25 (PC61), CD25 (7D4), Foxp3, and rat IgG1 detection on $CD4^+$ T cells in the immediate minutes and hours following *in vivo* administration of anti-CD25 (PC61). PC61 is a rat IgG1 isotype. *C,* representative analysis showing that following *in vivo* PC61 administration, rat IgG1 is found specifically on the surface of $GITR^+$ cells. Staining was done 10 days following antibody administration. Cervical lymph node is depicted. Gating is on $CD4^+$ lymphocytes. *D,* anti-CD25 blocks suppressive function. Mice were given 0.5 mg PC61 (anti-CD25) or isotype control antibody (control). After 5 days, spleens and cervical lymph nodes were removed and $CD4^+$ T cells isolated. Although CD25 was not seen on cells from anti-CD25– treated mice, GITR remained detectable at nearly the same levels and was used to sort $CD4^+GITR^-$ and $CD4^+GITR^+$ cells from these mice. The ability of these $CD4^+GITR^+$ cells to suppress the proliferation of $CD4^+CD25^-$ T cells from control mice was compared with that of T_{regs} isolated from control mice on the basis of either CD25 or CD25 and GITR expression. Whereas T_{regs} isolated from control mice suppressed T-cell proliferation in a dose-dependent fashion, $CD4^+GITR^+$ cells from anti CD25 treated mice did not.

$CD4^+Foxp3^+GITR^+$ cells that remained following PC61 administration represented the initial T_{reg} population. Furthermore, this population seemed to retain a level of surface CD25 that remained bound with the administered antibody, making CD25 detectable to 7D4, but not to PC61, anti-CD25 clones.

Given these findings, we examined whether the $CD4^+GITR^+$ cells present in mice that received anti-CD25 retained characteristic T_{reg} function *in vitro*. To this end, $CD4^+$ T cells were enriched by negative selection as above from VM/Dk mice 5 days following administration of either isotype control or anti-CD25 antibody. In the case of mice given anti-CD25, $CD4^+$ cells were sorted based on GITR expression, as this was the best remaining nonbound surface marker available for sorting. In control mice, $CD4^+$ cells were sorted based instead on expression of either CD25 (PC61) or both CD25 and GITR. The abilities of $CD4^+CD25^+$ and $CD4^+CD25^+GITR^+$ cells from control animals and $CD4^+GITR^+$ cells from anti-CD25–treated animals to suppress the proliferation of $CD4^+CD25^-$ responder T cells from control animals were then compared. (The testing of $CD4^+CD25^+GITR^+$ cells from control animals ensured that sorting based on GITR had no effect on suppressive function). Whereas $CD4^+CD25^+$ and $CD4^+CD25^+GITR^+$ cells from control animals suppressed T-cell proliferation to an equivalent extent, $CD4^+GITR^+$ cells from anti-CD25–treated animals failed to suppress the identical T-cell population (Fig. 4D).

Although it seems then that anti-CD25 administration *in vivo* does elicit a limited decline in T_{regs}, this depletion is clearly not comprehensive. Anti-CD25, however, does show the ability to functionally inactivate those T_{regs} that persist at significant levels *in vivo*, thereby interfering with their ability to suppress T-cell proliferation.

T-cell function and antiglioma immunity following anti-CD25 administration. As anti-CD25 administration did seem to affect T_{reg} function, we examined what effects systemic anti-CD25 administration might have on the general proliferative and IFN-γ-elaborating capacities of T cells isolated from VM/Dk mice. To this end, we removed the spleens of VM/Dk mice 7 days following either anti-CD25 or isotype control antibody administration. Lymphocyte-enriched populations were isolated and cultured with α-CD3- and α-CD28-coated latex beads as stimulators. The proliferative response of cells was measured by [^{3}H]thymidine uptake whereas IFN-γ elaboration was measured by ELISA. *In vivo* anti-CD25 significantly enhanced the ability of the lymphocyte compartment to proliferate (Fig. 5A) and secrete IFN-γ (Fig. 5B) in response to polyclonal T-cell receptor stimulation.

Experiments were subsequently initiated to determine the ability of anti-CD25 to enhance glioma-specific CTL responses. T cells were initially primed *in vivo* with a dendritic cell vaccine targeting malignant glioma. Mice were given antiCD25 or an isotype control antibody 4 days before receiving a single s.c. vaccination with syngeneic dendritic cells electroporated with total tumor RNA isolated from the SMA-560 glioma cell line (DC-SMA). Vaccinations were delivered bilaterally at the base of each ear, in proximity to the cervical lymph nodes.

Ten days pursuant to vaccination, spleens from all mice were harvested and restimulated *in vitro* with DC-SMA. Splenocytes were then entered into a CTL assay using SMA-560 cells ($H2K^b$) and two control tumor cell lines, B16/F10.9 ($H2K^b$) and EL4 ($H2K^b$), as targets. DC-SMA vaccination alone produced a significant specific lysis of SMA-560 targets. This CTL response, however, was dramatically enhanced in those mice that received anti-CD25 before vaccination, in which specific lysis of glioma targets approached 80% (Fig. 5C).

Survival and experimental allergic encephalitis studies. The strength of the effects of anti-CD25 on *in vitro* T-cell responses and CTL-mediated tumor cell lysis led us to test whether the same antibody would be a successful adjunct to a dendritic cell–based immunization strategy targeting glioma *in vivo*. We therefore examined the effects of anti-CD25 alone, dendritic cell vaccination alone, or a combination of both therapies on the ability of mice to reject intracranial glioma challenge.

To this end, all dendritic cells were electroporated with total tumor RNA isolated from the SMA-560 glioma cell line, and all mice were challenged with 10,000 SMA-560 cells placed intracranially under stereotactic guidance. Mice receiving anti-CD25 were given a single i.p. injection of PC61 antibody 4 days before vaccination whereas controls received an equivalent dose of isotype control antibody. Vaccines were delivered 7 days before tumor challenge and were injected s.c. at the base of each ear. Anti-CD25 as a lone modality extended median survival and proved capable of rejecting tumor in 50% of treated mice ($P = 0.0198$, in comparison with PBS group). Vaccine alone also produced significant survival benefits ($P = 0.0153$; median survival, 31 days versus 17 days in PBS group), but combining this strategy with anti-CD25 therapy significantly enhanced its efficacy ($P = 0.0486$ for comparison with vaccine only group), evoking complete tumor rejection in all treated mice and eliciting 100% long-term survival ($P = 0.0018$, in comparison of combination group with PBS group; Fig. 6A).

To convince ourselves of an immune-based mechanism for anti-CD25, we initiated a set of experiments to rule out a direct effect of anti-CD25 on the SMA-560 tumor. To begin, the SMA-560 cell line was tested for surface expression of CD25 by flow cytometry. No CD25 was detected (data not shown). Additionally, SMA-560 tumor cells were cultured in the presence of various doses of anti-CD25 antibody. No effects on either proliferation (Fig. 6B) or cell viability ($P = 0.9187$; Fig. 6C) were identified. Lastly, we examined the ability of anti-CD25 to elicit tumor rejection in immunocompromised mice. Anti-CD25 or isotype control antibody was administered *in vivo* in the same manner as above to athymic BALB/c mice, 4 days before intracranial challenge with 10,000 SMA-560 tumor cells. No effect on survival was elicited ($P = 0.1875$; Fig. 6D). Together, these data indicate the absence of a direct effect of anti-CD25 antibody on SMA-560 and suggest instead an immune-dependent mechanism of action.

Successful attempts to remove barriers to immunity against tumors situated within the CNS not infrequently carry risks for instigating autoimmune reactions similar to experimental allergic encephalomyelitis (26). Evidence supports an experimental allergic encephalitis-protective role for T_{regs} (27, 28), substantiating concerns associated with employing T_{reg} "depletion" as an adjunct to brain-tumor directed immunotherapy. As anti-CD25 then seemed to enhance immune responses to glioma in VM/Dk mice, we evaluated the risk that such strengthened antitumor immunity might pose concomitantly for the precipitation of experimental allergic encephalitis.

VM/Dk mice are a strain susceptible to experimental allergic encephalitis, such that autoimmunity can be evoked by a single

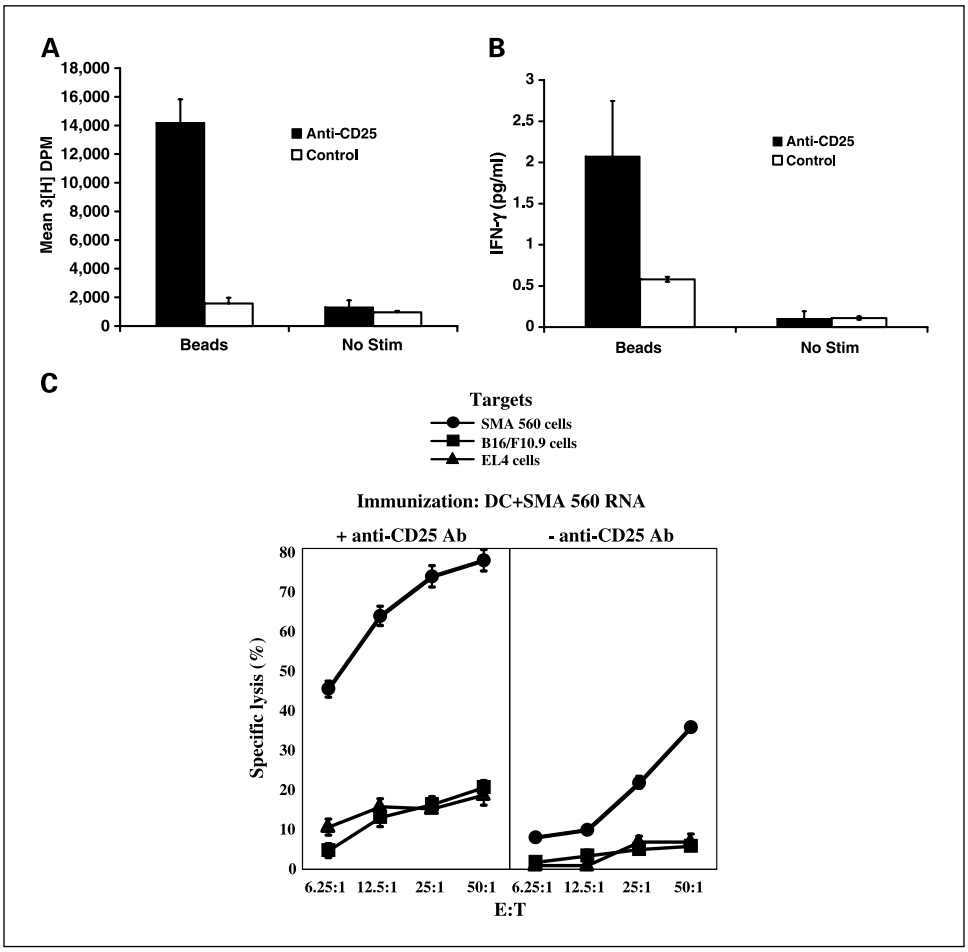

Fig. 5. Improved T-cell function following *in vivo* anti-CD25 administration. *A* and *B*, VM/Dk mice were given 0.5 mg PC61 (anti-CD25) or isotype control antibody (control). Five days later, lymphocytes from spleens were harvested and entered into proliferation assays (*A*) or IFN-γ elaboration assays (*B*). Cells were stimulated with latex beads coated with α-CD3 and α-CD28. Proliferation after 72 hours was assessed by [^{3}H]thymidine uptake. IFN-γ levels were assessed by ELISA. Columns, mean across triplicate wells; bars, SD. Comparisons between groups were made using unpaired *t* tests. Anti-CD25 enhanced lymphocyte proliferation by 900% ($P = 0.009$) and IFN-γ elaboration by 358% ($P = 0.019$). *C,* CTL assay. VM/Dk mice were once again treated with anti-CD25 (*left*) or isotype control antibody (*right*). All mice were primed 4 days later with DC-SMA vaccines, in which syngeneic dendritic cells had been loaded with total tumor RNA isolated from the SMA-560 glioma line. Vaccines were delivered s.c. at the base of each ear. Ten days later, spleens were harvested and entered into a europium-release CTL assay in which targets were SMA-560 cells (●) or two irrelevant tumor cell lines (■ and ▲; all targets were H2K^b). Points, mean percent specific lysis of triplicate platings for various effector/target (*E:T*) ratios; bars, SD. Vaccine alone produced significant specific lysis of SMA-560 targets (maximum, >30%) but the combination of vaccination and anti-CD25 elicited specific lysis that approached 80% ($P < 0.001$).

i.d. vaccination with MOG35-55 peptide in complete Freund's adjuvant (Fig. 6E and F). We therefore evaluated all mice in the above VM/Dk survival experiments for signs of experimental allergic encephalitis. No mice showed clinical signs of experimental allergic encephalitis and the absence of inflammation was confirmed histologically with staining of brain and spinal cord sections with H&E and luxol fast blue. Thus, anti-CD25 provided a powerful immune-based adjunct to dendritic cell vaccination and, despite being combined with a platform targeting shared tumor and CNS antigens, elicited no observable experimental allergic encephalitis in a susceptible mouse model.

Discussion

Cellular immune defects are frequently associated with malignancy and are particularly severe in patients with malignant glioma (18). Increased T_{reg} fractions among CD4$^+$ T cells have presently been shown in patients harboring a variety of malignancies and are believed to play a role in hindering antitumor immunity (13–16). In patients with malignant glioma, such increased fractions in peripheral blood have been shown to correlate with the manifestation of the cellular immune defects typical for these patients, including impaired T-cell proliferative responses and counterproductive shifts toward TH2 cytokine production (17). Given the immune impairments elicited by alterations to the T_{reg} fraction, an appropriate murine cancer model for exploring T_{reg}-directed interventions would be one in which similar alterations are aptly recapitulated. Thus, our studies here validate our murine model of malignant glioma as a suitable model for investigating means of manipulating the T_{reg} pool and exploring T_{reg} effects on antitumor immune function.

Specifically, we have found here that VM/Dk mice harboring syngeneic SMA-560 gliomas exhibit dramatic reductions in both CD4 and T_{reg} counts in the peripheral blood, spleens, and in the tumor ipsilateral and contralateral cervical lymph nodes, where these changes were most dramatic. This mirrors the situation observed in the peripheral blood of patients with malignant glioma, as does the relative persistence of T_{regs} as an increased fraction of the remaining CD4$^+$ T-cell compartment despite their reduced numbers. It also suggests the cervical lymph nodes as a potentially important site for immune analysis in patients with malignant glioma.

It is noteworthy, however, that this scenario of increased T_{reg} fractions and diminished CD4 and T_{reg} counts is not extrapolated into the bone marrow, which reveals instead an apparent true expansion of T_{reg} numbers in the tumor-bearing state despite harboring dramatic reductions in the T_{reg} fraction among CD4$^+$ cells. This apparent paradox is explained simply by the observation that an even larger expansion of the CD4$^+$CD25$^-$ compartment occurs in the marrow, drowning the T_{reg} increase. It is not yet clear whether these increases in CD4 and T_{reg} numbers represent a retention of these cells or,

more so, a selective trafficking to the marrow from other sites. Others have reported selective trafficking of memory $CD8^+$ T cells to the marrow in incidences of cancer (29, 30) but the observations here are unique and invite future study. We have suggested in the past that the CD4 compartment seems to "disappear" in patients with malignant glioma (17), but our findings here now provoke more appropriate discussions of tumor-induced alterations to the distributions of the CD4 and T_{reg} compartments.

One of our most salient findings is that anti-CD25 antibody, when given systemically, fails to eliminate $CD4^+Foxp3^+GITR^+$ cells from the peripheral blood, cervical lymph node, spleen, or bone marrow. A similar finding was very recently reported by Kohm et al. (25), who concluded after an eloquent study that T_{regs} remained in circulation following anti-CD25 mAb injection but that CD25 became undetectable on their surface, likely as a result of either receptor internalization or shedding. Based on the ability of anti-CD25 to exacerbate pathology in their model of acute experimental allergic encephalitis, the authors concluded that anti-CD25 must also interfere with T_{reg} function.

Our findings confirm and extend those of Kohm et al. albeit with some subtle differences to highlight. First, whereas our predecessors saw no decline in adoptively transferred T_{reg} numbers following anti-CD25 mAb administration, we analyzed physiologic T_{regs} and did detect a slow and moderate decrease in the number of $CD4^+Foxp3^+GITR^+$ cells in the time following anti-CD25 injection. This was seen at a variety of sites tested. Although it remains possible that an unprecedented population of $CD4^+Foxp3^+GITR^+$ cells arose *de novo* instead of depleted $CD25^+$ cells, a number of our results argue strongly against this.

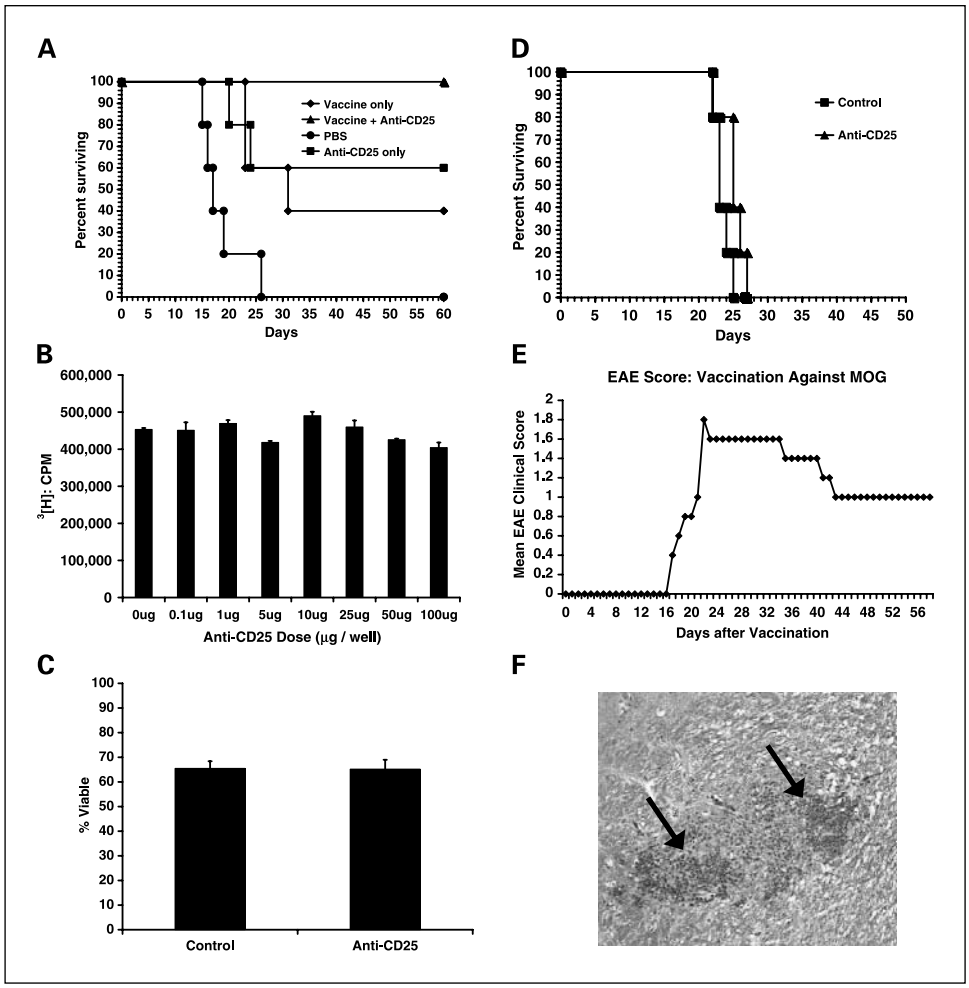

Fig. 6. Systemic anti-CD25 enhances antitumor immunity *in vivo* without eliciting experimental allergic encephalitis. *A,* combination of anti-CD25 and dendritic cell vaccine produces 100% survival following intracranial tumor challenge. VM/Dk mice ($n = 5$ per group) were given 0.5 mg PC61 (anti-CD25) or isotype control antibody i.p. on day −10. On day −7, mice were vaccinated with 2.5×10^5 dendritic cells electroporated with total tumor RNA from the SMA-560 glioma cell line or injected with an equivalent volume of PBS. Injections were delivered s.c. at the base of each ear. On day 0, all mice were challenged i.c. with 10,000 syngeneic SMA-560 cells. Kaplan-Meier survival data are presented as the percentage of mice surviving in each group. Differences in survival were determined by log-rank test. Anti-CD25 ($P = 0.0198$) and dendritic cell vaccine ($P = 0.0153$) alone each produced significant survival benefits, but the combination of the two elicited 100% long-term survival ($P = 0.0018$). *B* and *C,* anti-CD25 has no direct antitumor effect *in vitro*. SMA-560 cells were cultured in the presence of various doses of anti-CD25 for 3 days; after which, proliferation was assessed by [^{3}H]thymidine uptake (*B*) and viability was assessed by Annexin V and propidium iodide staining (*C*). No significant effects were encountered. *D,* anti-CD25 delivered systemically to athymic BALB/c mice fails to protect against tumor challenge. Athymic mice were challenged intracranially as above with 10,000 SMA-560 tumor cells 4 days following i.p administration of either anti-CD25 or isotype control antibody. No survival benefit was conferred ($P = 0.1875$). *E* and *F,* VM/Dk mice are susceptible to experimental allergic encephalitis, which develops following a single i.d. injection with MOG35-55. *E,* mean clinical experimental allergic encephalitis scores following MOG35-55 injection. *F,* representative experimental allergic encephalitis – positive histology from an affected spinal cord. Histologic staining is with H&E and luxol fast blue. Arrows, focused areas of lymphocytic infiltrate.

First, we observed a precipitous drop in $CD25^+$ (PC61) cells and no change in the levels of $CD4^+Foxp3^+GITR^+$ cells in the immediate minutes and hours following anti-CD25 injection. Furthermore, our persistent ability to detect both the administered antibody (a rat IgG1 isotype) and an alternative epitope of CD25 (7D4) specifically on the surface of $CD4^+Foxp3^+GITR^+$ cells insinuates that these were indeed the same cells and that CD25 was neither entirely shed nor internalized, with at least some amount remaining on the cell surface bound by antibody. The continued presence of the anti-CD25 rat IgG1 on these cells may have effectively blocked CD25 detection and may also have been the impetus for an inefficient antibody-dependent cell-mediated cytotoxicity–based depletion. This would likewise explain the slow but somewhat steady decline in $CD4^+Foxp3^+GITR^+$ cell number following anti-CD25 mAb injection.

We also provide a more direct demonstration that anti-CD25 administered *in vivo* may explicitly interfere with T_{reg} function. Within 5 days of mAb injection, we established that when the remaining $CD4^+GITR^+$ cells were isolated, they no longer possessed the suppressive function shown by $GITR^+$ cells in naïve mice. Together with those by Kohm et al., these findings dramatically alter our understanding of how anti-CD25 may work to enhance immune responses. New studies into similar reagents available clinically, their mechanisms of action and their limitations for employment (such as the potential for interference with activated $CD25^+$ T cells), are warranted.

Despite the paradigm shift, however, our results in this model show the safety and utility of an anti-CD25 strategy for the improvement of glioma-directed immunotherapy. Given resilient notions of CNS immune privilege (31–33), the ability to generate a systemic antitumor immune response that is capable of extending itself into the CNS remains as a coveted goal of brain tumor immunotherapy. We find that systemic anti-CD25 mAb enhances T-cell proliferation and IFN-γ elaboration, strengthens antigen-specific anti-glioma CTL responses, and, most importantly, dramatically improves survival rates in a murine model of intracranial glioma without eliciting experimental allergic encephalitis. An immune-based mechanism for anti-CD25 is suggested, as the antibody fails to elicit direct antitumor effects or to eliminate tumor in immunocompromised athymic mice. Furthermore, the moderate survival benefit provided by anti-CD25 alone in our model (i.e., without pursuant dendritic cell vaccination) suggests that a spontaneous systemic physiologic immune response capable of targeting tumors in the CNS exists, and that peripheral T_{regs} are important in attenuating this response.

Acknowledgments

We thank John F. Whitesides, Patrice McDermott, and Danielle King (Duke Human Vaccine Institute Flow Cytometry Core Facility) for their technical assistance.

References

1. Green DR, Webb DR. Saying the "S" word in public. Immunol Today 1993;14:523–5.
2. Sakaguchi S, Sakaguchi N, Asano M, Itoh M, Toda M. Immunologic self-tolerance maintained by activated T cells expressing IL-2 receptor α-chains (CD25). Breakdown of a single mechanism of self-tolerance causes various autoimmune diseases. J Immunol 1995;155:1151–64.
3. Asano M, Toda M, Sakaguchi N, Sakaguchi S. Autoimmune disease as a consequence of developmental abnormality of a T cell subpopulation. J Exp Med 1996;184:387–96.
4. Salomon B, Lenschow DJ, Rhee L, et al. B7/CD28 costimulation is essential for the homeostasis of the $CD4^+CD25^+$ immunoregulatory T cells that control autoimmune diabetes. Immunity 2000;12:431–40.
5. Stephens GL, McHugh RS, Whitters MJ, et al. Engagement of glucocorticoid-induced TNFR family-related receptor on effector T cells by its ligand mediates resistance to suppression by $CD4^+CD25^+$ T cells. J Immunol 2004;173:5008–20.
6. Taguchi O, Nishizuka Y. Self tolerance and localized autoimmunity. Mouse models of autoimmune disease that suggest tissue-specific suppressor T cells are involved in self tolerance. J Exp Med 1987;165:146–56.
7. Taguchi O, Kontani K, Ikeda H, Kezuka T, Takeuchi M, Takahashi T. Tissue-specific suppressor T cells involved in self-tolerance are activated extrathymically by self-antigens. Immunology 1994;82:365–9.
8. Seddon B, Mason D. Regulatory T cells in the control of autoimmunity: the essential role of transforming growth factor β and interleukin 4 in the prevention of autoimmune thyroiditis in rats by peripheral CD4(+)CD45RC(−) cells and CD4(+)CD8(−) thymocytes. J Exp Med 1999;189:279–88.
9. Bagavant H, Thompson C, Ohno K, Setiady Y, Tung KS. Differential effect of neonatal thymectomy on systemic and organ-specific autoimmune disease. Int Immunol 2002;14:1397–406.
10. Fontenot JD, Gavin MA, Rudensky AY. Foxp3 programs the development and function of $CD4^+CD25^+$ regulatory T cells. Nat Immunol 2003;4:330–6.
11. Khattri R, Cox T, Yasayko SA, Ramsdell F. An essential role for Scurfin in $CD4^+CD25^+$ T regulatory cells. Nat Immunol 2003;4:337–42.
12. Somasundaram R, Jacob L, Swoboda R, et al. Inhibition of cytolytic T lymphocyte proliferation by autologous $CD4^+/CD25^+$ regulatory T cells in a colorectal carcinoma patient is mediated by transforming growth factor-β. Cancer Res 2002;62:5267–72.
13. Curiel TJ, Coukos G, Zou L, et al. Specific recruitment of regulatory T cells in ovarian carcinoma fosters immune privilege and predicts reduced survival. Nat Med 2004;10:942–9.
14. Ichihara F, Kono K, Takahashi A, Kawaida H, Sugai H, Fujii H. Increased populations of regulatory T cells in peripheral blood and tumor-infiltrating lymphocytes in patients with gastric and esophageal cancers. Clin Cancer Res 2003;9:4404–8.
15. Liyanage UK, Moore TT, Joo HG, et al. Prevalence of regulatory T cells is increased in peripheral blood and tumor microenvironment of patients with pancreas or breast adenocarcinoma. J Immunol 2002;169:2756–61.
16. Woo EY, Chu CS, Goletz TJ, et al. Regulatory CD4(+)CD25(+) T cells in tumors from patients with early-stage non-small cell lung cancer and late-stage ovarian cancer. Cancer Res 2001;61:4766–72.
17. Fecci PE, Mitchell DA, Whitesides JF, et al. Increased regulatory T-cell fraction amidst a diminished CD4 compartment explains cellular immune defects in patients with malignant glioma. Cancer Res 2006;66:3294–302.
18. Dix AR, Brooks WH, Roszman TL, Morford LA. Immune defects observed in patients with primary malignant brain tumors. J Neuroimmunol 1999;100:216–32.
19. McHugh RS, Shevach EM. Cutting edge: depletion of $CD4^+CD25^+$ regulatory T cells is necessary, but not sufficient, for induction of organ-specific autoimmune disease. J Immunol 2002;168:5979–83.
20. Kohm AP, Williams JS, Miller SD. Cutting edge: ligation of the glucocorticoid-induced TNF receptor enhances autoreactive $CD4^+$ T cell activation and experimental autoimmune encephalomyelitis. J Immunol 2004;172:4686–90.
21. Onizuka S, Tawara I, Shimizu J, Sakaguchi S, Fujita T, Nakayama E. Tumor rejection by *in vivo* administration of anti-CD25 (interleukin-2 receptor α) monoclonal antibody. Cancer Res 1999;59:3128–33.
22. Shimizu J, Yamazaki S, Sakaguchi S. Induction of tumor immunity by removing $CD25^+CD4^+$ T cells: a common basis between tumor immunity and autoimmunity. J Immunol 1999;163:5211–8.
23. Steitz J, Bruck J, Lenz J, Knop J, Tuting T. Depletion of CD25(+) CD4(+) T cells and treatment with tyrosinase-related protein 2-transduced dendritic cells enhance the interferon α-induced, CD8(+) T-cell-dependent immune defense of B16 melanoma. Cancer Res 2001;61:8643–6.
24. Sutmuller RP, van Duivenvoorde LM, van Elsas A, et al. Synergism of cytotoxic T lymphocyte-associated antigen 4 blockade and depletion of CD25(+) regulatory T cells in antitumor therapy reveals alternative pathways for suppression of autoreactive cytotoxic T lymphocyte responses. J Exp Med 2001;194:823–32.
25. Kohm AP, McMahon JS, Podojil JR, et al. Cutting edge: anti-CD25 monoclonal antibody injection results in the functional inactivation, not depletion, of $CD4^+CD25^+$ T regulatory cells. J Immunol 2006;176:3301–5.
26. Rivers TM, Schwentker FF. Encephalomyelitis accompanied by myelin destruction experimentally produced in monkeys. J Exp Med 1935;61:689–702.
27. Kohm AP, Carpentier PA, Anger HA, Miller SD. Cutting edge: $CD4^+CD25^+$ regulatory T cells suppress antigen-specific autoreactive immune responses and

central nervous system inflammation during active experimental autoimmune encephalomyelitis. J Immunol 2002;169:4712–6.
28. Hori S, Haury M, Coutinho A, Demengeot J. Specificity requirements for selection and effector functions of $CD25^{+}4^{+}$ regulatory T cells in anti-myelin basic protein T cell receptor transgenic mice. Proc Natl Acad Sci U S A 2002;99:8213–8.
29. Letsch A, Keilholz U, Assfalg G, Mailander V, Thiel E, Scheibenbogen C. Bone marrow contains melanoma-reactive $CD8^{+}$ effector T cells and, compared with peripheral blood, enriched numbers of melanoma-reactive $CD8^{+}$ memory T cells. Cancer Res 2003;63:5582–6.
30. Beckhove P, Feuerer M, Dolenc M, et al. Specifically activated memory T cell subsets from cancer patients recognize and reject xenotransplanted autologous tumors. J Clin Invest 2004;114:67–76.
31. Medawar PB. Immunity to homologous grafted skin: III. The fate of skin homografts transplanted to the brain, to subcutaneous tissue, and to the anterior chamber of the eye. Br J Exp Pathol 1948;29:58–69.
32. Parney IF, Hao C, Petruk KC. Glioma immunology and immunotherapy. Neurosurgery 2000;46:778–91.
33. Fabry Z, Raine CS, Hart MN. Nervous tissue as an immune compartment: the dialect of the immune response in the CNS. Immunol Today 1994;15:218–24.